https://doi.org/10.15407/ujpe67.4.240

O.K. SHUAIBOV, O.Y. MINYA, A.O. MALININA, R.V. GRYTSAK, O.M. MALININ

Uzhhorod National University

(3, Narodna Sq., Uzhhorod, Ukraine; e-mail: alexsander.shuaibov@uzhnu.edu.ua)

OPTICAL CHARACTERISTICS AND PARAMETERS OF OVERSTRESSED NANOSECOND DISCHARGE PLASMA IN ARGON BETWEEN ALUMINUM AND CHALCOPYRITE

The optical characteristics and parameters of overstressed nanosecond discharges in argon between aluminum and chalcopyrite ($CuInSe_2$) electrodes at the argon pressures $p(Ar) = 13.3$ and 101 kPa have been determined. Due to microexplosions of natural inhomogeneities located on the working electrode surfaces in a strong electric field, both aluminum and chalcopyrite vapors are introduced into plasma, which creates preconditions for the synthesis of quaternary chalcopyrite ($CuAlInSe_2$) thin films beyond the discharge. Voltage pulses across the discharge interval $d = 1 \times 10^{-3}$ m, current pulses, and pulse energy contribution to plasma are analyzed. The spectra of plasma radiation emission have been studied in detail, which made it possible to identify the main decay products of chalcopyrite molecules and the energy states of the atoms and single-charged ions of aluminum, copper, and indium that had been formed at the discharge. The reference spectral lines of aluminum, copper, and indium atoms and ions have been detected, which can be used to control the sputtering process of thin quaternary chalcopyrite films. Using the numerical simulation of the parameters of overstressed nanosecond-discharge plasma created on the basis of aluminum and chalcopyrite vapors and by solving the Boltzmann kinetic equation for the electron energy distribution function, the electron temperature and concentration in the discharge and specific discharge power losses, as well as their dependences on the ratio E/N the electric field strength E and the total concentration N of components in the aluminum and argon vapor mixture, are calculated.

K e y w o r d s: overstressed nanosecond discharge, aluminum, chalcopyrite, argon.

1. Introduction

In the vast majority of cases, plasma of spark discharges in gases contains atoms and ions of electrodes' materials, which can be used to synthesize metal and semiconductor nanostructures on dielectric substrates arranged beyond the discharge region [1, 2]. Therefore, it is important to perform a thorough research of plasma parameters for such discharges in order to determine a relation between them and the parameters of synthesized nanostructured films.

In particular, the results concerning time-changes in the radiation emission spectra of spark discharge plasma in the air gap between aluminum electrodes were presented in work [3]. Two maxima were observed in the oscillograms of the radiation intensity of the spectral lines of the electrode material [aluminum atoms (Al I), single-charge aluminum ions (Al II), and double-charge aluminum ions (Al III)]. The main diagnostic spectral lines of aluminum were those at 394.3 nm Al I, 281.6 and 283.13 nm Al II, and 371.3 nm Al III). The afterglow duration at the aluminum atom transitions reached 600 μs. Therefore, the cited authors have suggested the recombination

mechanism for the population of excited energy levels of atoms and single-charged aluminum ions.

The main characteristics of the 25–70-ns spark discharge were quoted in work [4]. The discharge between two cylindrical electrodes fabricated of brass or stainless steel and located at the distance $d = (1 \div 15) \times 10^{-3}$ m from each other was ignited by means of two different high-voltage pulse generators with pulse durations of 25 and 65–70 ns. In the case of brass electrodes separated by the distance $d = 5 \times 10^{-3}$ m, the main radiation in the radiation spectrum of plasma was concentrated in a spectral interval of 200–230 nm. The identification of the spectrum and the nature of its emitters was not performed in work [4]. Later, we found [1, 5] that most of those spectral lines belong to the atom and single-charged ion of copper.

The results obtained for the spectral and temporal characteristics of the pulse-periodic nanosecond discharge in nitrogen with a beam of runaway electrons were presented in work [6]. In these experiments, aluminum electrodes of the "needle-plane" type and arranged at the interelectrode distances $d = 2 \times 10^{-3}$ and 6×10^{-3} m were applied. For the discharge at $d = 2 \times 10^{-3}$ m, colored mini-jets of plasma based on aluminum vapor plasma were observed in the discharge near the cathode tip. The most intensive spectral Al I and Al II lines were observed in the plasma radiation spectra at 396.4, 396.12, 622.62, 623.17. 704.21, 705.66, and 706.36 nm, respectively. The analysis of oscillograms of plasma glowing at Al I and Al II transitions showed that they have a recombination origin.

The work [7] contains the results of a research dealing with UV radiation of high-voltage pulsed multielectrode surface discharge in air of atmospheric pressure. The discharge was ignited in the form of a set of successive microplasma formations with a specific energy contribution at a level of 10^{-3} J/m^3. In plasma radiation, the radiation by atoms and ions of electrode material dominated. This source was the most effective when the interelectrode distance was $d = 1.5 \times 10^{-3}$ m in a system of six equal gaps, i.e., when the voltage overstress across the discharge gap was maximum. The total energy introduced into the discharge was about 0.2 J.

Besides the plasma of aluminum vapor, vapor of the materials of other electrodes were also successfully introduced into the discharge gap of overstressed nanosecond discharge. In particular, in works [9, 10], the optical characteristics of the plasma of copper and iron vapors were reported. Blue jets were generated in the nitrogen-based discharge when the cathode is made of stainless steel. For the copper cathode, green jets were generated at gas pressures of 4.4 and 6.7 kPa. For the aluminum cathode, the jets were blue. The appearance of these plasma jets is associated with the explosions of micro-inhomogeneities on the cathode surface and metal electroerosion giving rise to the formation of metal vapor that filled the discharge gap.

The study of the radiation spectra of nanosecond discharge in nitrogen at pressures of 13.3–26.6 kPa showed that plasma from the central part of discharge gap emits only intensive bands of nitrogen molecule. In the case of contracted discharge in air at a pressure of 26.6 kPa, a characteristic broadband continuum in a wavelength interval of 200–800 nm, the spectral lines of nitrogen ions (N II), the lines of oxygen atom, and the bands of NO radical were registered [9]. In plasma around the cathode tip, radiation by Al I, Fe I, and Fe II ions dominated. Intensive spectral lines of aluminum atoms at wavelengths of 394.4 and 394.15 nm were observed at that, for which the upper energy level at 3.14 eV was common, whereas the lower levels were either ground or lower on the energy scale ($E = 0.014$ eV) [10].

The work [11] contains the results of a study of thin-film solar cells based on $CuIn_{1-x}Al_xSe_2$. The best solar cells synthesized in this way have an efficiency of about 6.5% if the ratio between the aluminum and the total indium + aluminum contents, Al/(In + Al), equals 0.2. A comparison of those values with similar data obtained for aluminum-free devices showed a significant growth of the efficiency of the former. These data confirmed a substantial improvement in the efficiency of the device associated with the increase in the band gap size of absorber in such quaternary alloys. Therefore, it is important to develop new physical gas-discharge methods aimed at the synthesis of quaternary chalcopyrites on the basis of Cu, In, Al and Se in the form of thin films, which can be produced making use of overstressed nanosecond discharge between aluminum electrodes and the corresponding ternary chalcopyrite ($CuInSe_2$).

In this paper, we present the results obtained while studying the characteristics of overstressed nanosecond discharge plasma in argon between two electrodes

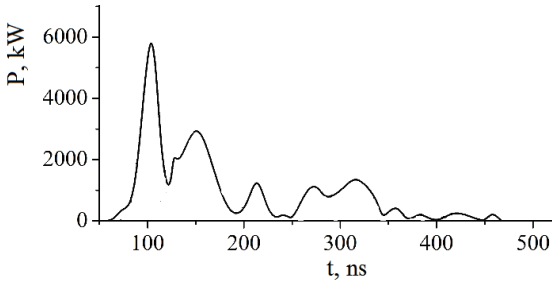

Fig. 1. Pulsed power of overstressed nanosecond discharge between two chalcopyrite electrodes at $p(\mathrm{Ar}) = 101$ kPa

made of aluminum, two electrodes made of chalcopyrite, and between an electrode made of aluminum and an electrode made of chalcopyrite. In particular, the parameters of the studied discharge plasma are reported, which were determined by solving the Boltzmann kinetic equation for the electron energy distribution function in the case of homogeneous plasma containing simultaneously both aluminum and chalcopyrite vapors.

2. Experimental Technique and Electrical Characteristics

Overstressed nanosecond discharge between an aluminum electrode and a chalcopyrite electrode ($CuInSe_2$) was ignited in a vacuum discharge chamber made of plexiglass. The scheme of discharge device and the device for film deposition was given in works [8, 12, 13]. The distance between the electrodes was 1×10^{-3} m. The discharge chamber was pumped out making use of a pre-vacuum pump to a residual air pressure of 10 Pa; then argon was inlet into the chamber. The argon pressure was 13.3 or 101 kPa. The diameter of the cylindrical electrodes was 5×10^{-3} m. The radius of the rounded working lectrode-end surface was identical and equal to -1.5×10^{-3} m.

Oscillograms of voltage pulses across the discharge gap and oscillograms of current pulses were registered using a broadband capacitive voltage divider, a Rogovsky belt, and a broadband oscilloscope 6LOR-04 with a time resolution of 1–2 ns.

To register plasma radiation spectra, an MDR-2 monochromator and a photomultiplier FEU-106 were applied. A signal from the photomultiplier was fed to the amplifier and fixed on a personal computer display using an amplitude-to-digital converter in an automated spectrum measurement system. Discharge radiation was examined in a spectral interval of 200–650 nm.

Test experiments in argon were performed using a discharge between two electrodes made of chalcopyrite or two aluminum electrodes installed instead of them. The interelectrode distance was 1×10^{-3} m in both cases, which allowed us to achieve a substantial overstress across the discharge gap. In both cases, the discharge was spatially uniform owing to preionization of the gaseous medium by accompanying X-rays and a beam of electrons escaping from plasma [14]. The discharge volume depended on the frequency of voltage pulses. The "point discharge" mode was achieved only at the repetition frequency of voltage pulses in the interval $f = 40 \div 150$ Hz. When the frequency was increased to 1000 Hz, the plasma volume in the gas-discharge emitter increased from 10^{-8} to 10^{-7} m^3.

The oscillograms of voltage and current pulses in discharges between two chalcopyrite or two aluminum electrodes at an air pressure of 101 kPa were presented in works [13, 15]. The voltage and current oscillograms had the form of time-damping oscillations lasting about 7–10 ns, which was associated with a mismatch between the output resistance of high-voltage modulator and the load resistance. As the interelectrode distance was increased from 1 to 5 mm, the resistance matching became better and the number of oscillations in the voltage and current pulses decreased. However, this mode was not optimal for the formation of flows of electrode-material-based plasma, as well as the high-voltage subnanosecond discharge between aluminum electrodes [6]. The maximum voltage amplitude reached 40–60 kV, and the current amplitude 120–150 A (for chalcopyrite electrodes). For the overstressed nanosecond discharge between aluminum electrodes ($d = 1 \times 10^{-3}$ m) under an argon pressure of 101 kPa, the maximum oscillation magnitude reached 35–40 V for the voltage, and up to 250 A for the current.

Figures 1 and 2 illustrate the pulse power of discharge in argon between two chalcopyrite and two aluminum, respectively, electrodes ($d = 1 \times 10^{-3}$ m, $p(\mathrm{Ar}) = 101$ kPa). The main fraction of the pulsed electric power was introduced into plasma within the first 150–200 ns and reached 5–6 MW (chalcopyrite electrodes).

Graphical integration of the pulse power over the time made it possible to determine the energy of

one discharge pulse introduced into plasma. In particular, the energy contribution to the overstressed nanosecond discharge between chalcopyrite electrodes reached 0.400 J (p(Ar) = 101 kPa). For the discharge between aluminum electrodes, it was 0.441 J (Fig. 2).

At p(Ar) = 13.3 kPa (Fig. 3), the mismatch between the output resistance of hight-voltage modulator and the resistance of nanosecond discharge plasma between the aluminum and semiconductor ($CuInSe_2$) electrodes was the largest. Therefore, the total duration of voltage oscillations across the gap and discharge current oscillations reached 450–500 ns, with the duration of separate oscillations reaching 7–70 ns. Short-term oscillations were best observed in the voltage oscillograms. They were absent from the current oscillograms because to a large time constant of the Rogovsky belt used in this experiment. The maximum value of the voltage drop across the discharge gap was 10–12 kV, if the positive and negative voltage pulse amplitudes are taken into account. The maximum current amplitude reached 200 A at the initial stage of discharge burning. The maximum value of the discharge pulsed power was attained within the first 100 ns from the ignition time and amounted to 450–500 kW.

As the argon pressure increased to 101 kPa, the plasma resistance increased and the resistance matching with the high-voltage bipolar pulse modulator became better. In this case, the maximum amplitude of the voltage amplitude increased to 60 kV and the duration of the main part of the voltage oscillogram diminished to 100 ns. The maximum amplitude of the current pulse reached 180–200 A and its total duration was 400–500 ns. Perhaps, the diffuse discharge survived only within the first 100–120 ns and then it transformed into the contracted state. The maximum value of the discharge pulsed power was observed within the first 130 ns after its ignition and was equal to 4 MW. An increase of argon pressure from 13.3 to 101.3 kPa led to the growth in the energy of a single electric pulse from 0.046 to 0.423 J (Figs. 3 and 4).

3. Optical Characteristics

Test studies of plasma radiation spectra were carried out for the overstressed nanosecond discharge in argon between either two electrodes made of aluminum

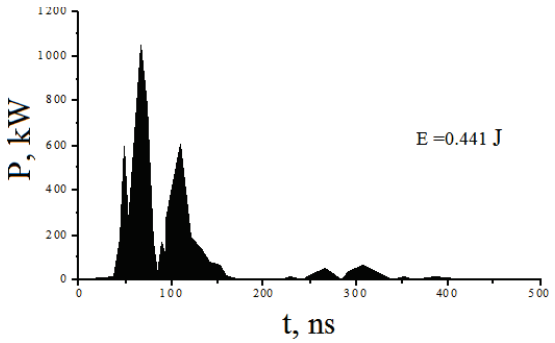

Fig. 2. Pulsed power of overstressed nanosecond discharge between two aluminum electrodes. $d = 1 \times 10^{-3}$ m, p(Ar) = = 101 kPa

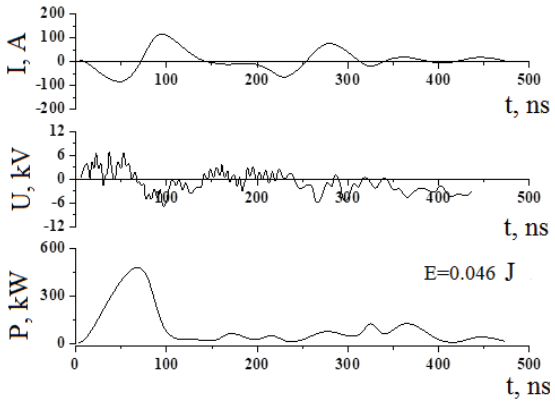

Fig. 3. Oscillograms of the current, voltage, and pulse power of overstressed nanosecond discharge between electrodes made of aluminum and $CuInSe_2$. p(Ar) = 13.3 kPa

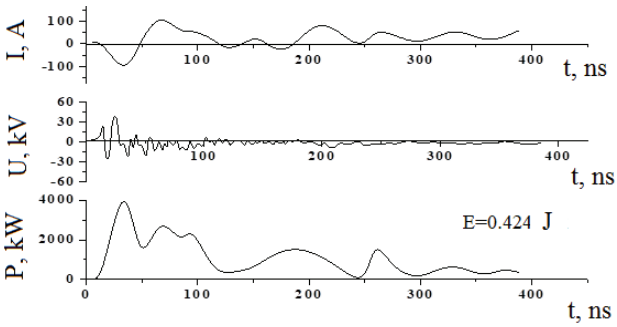

Fig. 4. The same as in Fig. 3, but for p(Ar) = 101 kPa

(Fig. 5) or two electrodes made of the $CuInSe_2$ compound (Fig. 6). When identifying spectral lines in the spectra, reference books [16–18] were used. At an argon pressure of 13.3 kPa, two groups of aluminum-atom (Al I) spectral lines prevailed in the discharge radiation spectrum: at 308.21, 309.27, and 309.28 nm

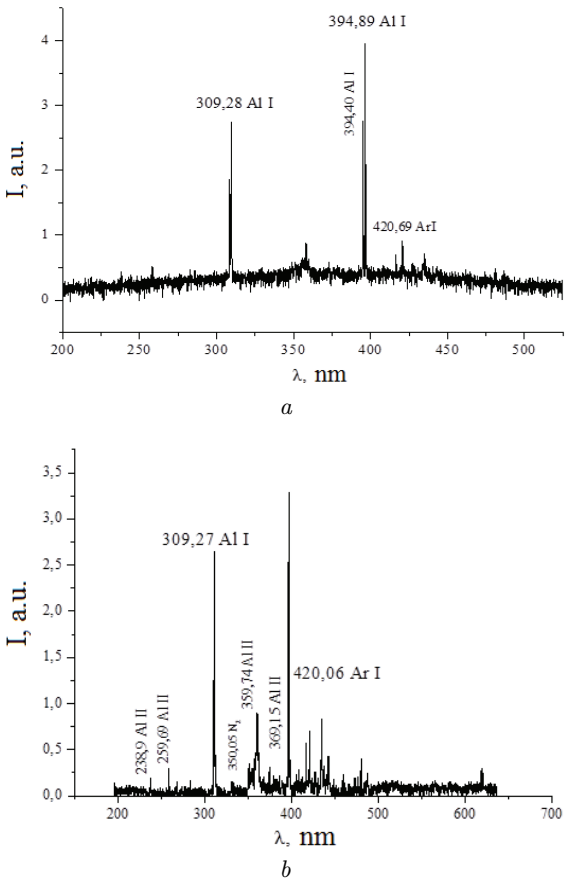

Fig. 5. Radiation spectra of overstressed nanosecond discharge plasma between aluminum electrodes at $p(\mathrm{Ar}) = 13.3$ (a) and 101 kPa (b)

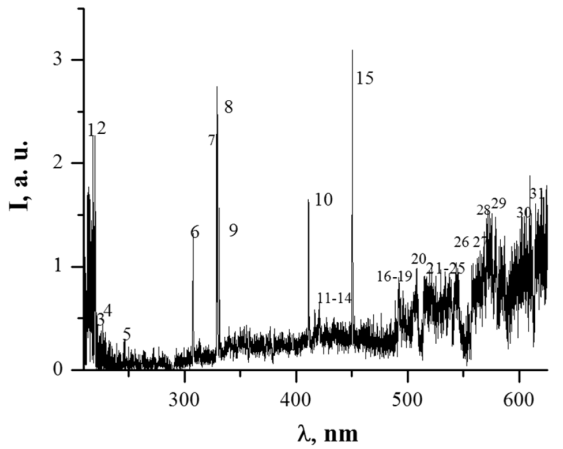

Fig. 6. Radiation spectrum of overstressed nanosecond discharge plasma between two chalcopyrite electrodes. $p(\mathrm{Ar}) = 101$ kPa

and at 394.40, 394.89, and 396.15 nm. Less intensive were the spectral lines 415.85, 419.83, and 420.06 nm Al I. The lower energy level of the spectral lines 308.21 and 394.40 nm (resonance) Al I is the ground state of aluminum atom, and the energies of their upper states are 4.02 and 3.14 eV, respectively. The spectral lines 309.27 and 309.28 nm Al I terminate at a low energy level with an energy of 0.014 eV. The upper energy levels for the lines 415.85, 419.83,and 420.06 nm Al I are within an interval of 14.499–14.529 eV, and the lower ones within an energy interval of 11.548–11.624 eV.

Figure 6 exhibits the radiation emission spectrum of overstressed nanosecond discharge between chalcopyrite electrodes at an argon pressure of 101.3 kPa. The results of identification of the main spectral lines and bands of the decay products of the chalcopyrite molecule, as well as a thorough analysis of the spectrum, were given in work [13]. However, the main feature of the spectrum shown in Fig. 6 it should be pointed out. The most intensive in the spectrum were the spectral lines of copper and indium atoms and ions, which were observed against the background of continuous plasma radiation. The origin of continuous plasma radiation may be associated with thermal or recombination plasma radiation. Copper and indium atoms are least bound oned in the chalcopyrite molecule, which was the main component of massive electrodes [19]. Therefore, the linear section of the plasma radiation spectrum is mainly produced by separate spectral lines of copper and indium atoms and single-charged ions both for laser plasma formed in vacuum at the surface of the target made of this compound [20] and for gas discharge plasma on the basis of air, nitrogen, or argon for overstressed nanosecond discharge between copper electrodes under atmospheric pressure [21]. The radiation emission spectrum of the gaseous component, argon, did not manifest itself in this spectral interval.

The radiation spectra and the results of identification of the most intensive spectral lines of the aluminum atom and single-charged ion, as well as the molecular bands, the decay products of chalcopyrite molecules in overstressed nanosecond discharge between aluminum and chalcopyrite electrodes at $p(\mathrm{Ar}) = 101$ and 13.3 kPa are depicted in Figs. 7 and 8 and in Tables 1 and 2.

At an argon pressure of 101 kPa, the most short-wavelength and most intensive section of the spec-

trum in the radiation spectrum of plasma based on the mixture of aluminum and chalcopyrite vapors (lines *1–10*) included the spectral lines of copper and aluminum atoms and single-charged ions. The spectral lines were densely spaced against the continuum background and practically formed a band extending over 50 nm (from 200 to 250 nm).

The second group of spectral lines, which were also observed against the continuous radiation background in a spectral interval of 308–451 nm, had a higher separation degree, but their intensities were low. Besides the spectral lines of copper and aluminum atoms and single-charged ions, separate lines of argon atom (Ar I) and argon ion (Ar II) were also observed in the violet and blue spectral intervals. Of the indium lines, only atomic spectral lines at 410.17 and 451.13 nm appeared in the radiation spectrum.

In a spectral interval of 450–650 nm, the intensity of continuous radiation increased strongly with the increasing radiation wavelength. The spectral lines of argon and copper atoms were mainly observed against the continuous radiation background. The main reason for the appearance of intensive continuum in the spectrum is the transition of the diffuse form of overstressed nanosecond discharge into the contracted state (spark) under the argon atmospheric pressure.

A reduction of the argon pressure to 13.3 kPa favored the discharge ignition in the diffuse form, whereas the contraction was much less pronounced. Those changes led to a better manifestation of separate spectral lines of copper, aluminum, and argon atoms and single-charged ions in the radiation spectrum (Fig. 8). The intensity for the group of copper and aluminum spectral lines in a wavelength interval of 200–225 nm (lines *1–6*) decreased by a factor of four. At reduced argon pressures, the most intensive and well-separated were spectral lines *7–18* within a wavelength interval of 230–400 nm. The intensity of continuous radiation in this spectral range was minimum. Here, the most intensive were the spectral lines *11* (308.21 nm Al I, the resonance spectral line), *12* (309.27 nm Al I), *17* (394.40 nm Al I), and *18* (396.1 nm Al I). Other spectral lines within this spectral interval mainly belonged to copper and aluminum atoms.

Another rather well-separated group of spectral lines *19–33* was emitted in a wavelength interval of 400–500 nm. It included the spectral lines of argon

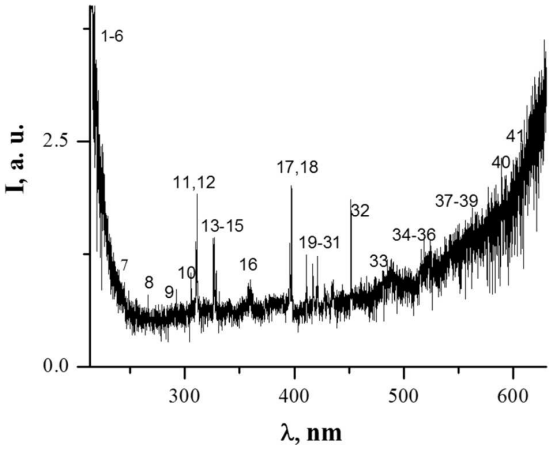

Fig. 7. Radiation spectrum of overstressed nanosecond discharge plasma between aluminum and chalcopyrite electrodes. $p(\mathrm{Ar}) = 101$ kPa

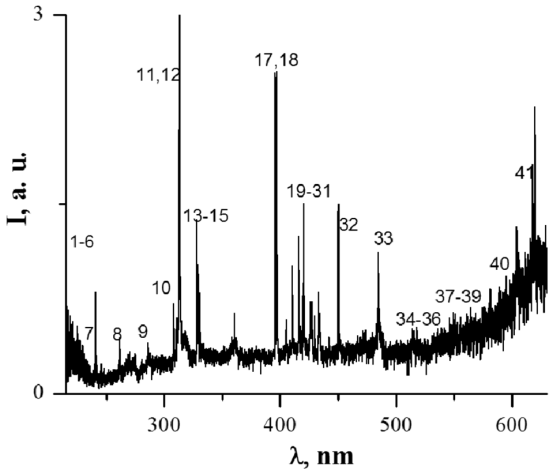

Fig. 8. The same as in Fig. 7, but for $p(\mathrm{Ar}) = 13.3$ kPa

atom and single-charge ion and the spectral lines 451.13 nm In I, and 484.22, 515.83 nm Cu I.

In a spectral interval of 500–630 nm prevailed continuous radiation (probably, thermal radiation of plasma), with the spectral lines 594.92 and 603.21 nm Ar I being pronounced against it.

As the argon pressure grew from 13.3 to 101.3 kPa, the intensities of the spectral lines of copper and indium atoms and their single-charge ions increased. In particular, the maximum growth was found for the intensity of the spectral line 218.17 nm Cu I (8.6 times), the lower energy level for which is the ground energy level of copper atom. An intensity increase of 6.3 times was registered for the ionic line 219.56 nm

Table 1. **Identification of the most intensive spectral lines of aluminum atom and single-charged ion, as well as the molecular bands of decay products of the chalcopyrite molecule in overstressed nanosecond discharge at $p(\mathrm{Ar}) = 101$ kPa**

No.	$\lambda_{\mathrm{tab.}}$, nm	I_{exp}, a.u	Object	$E_{\mathrm{low.}}$, eV	$E_{\mathrm{up.}}$, eV	$\mathrm{Lover}_{\mathrm{term}}$	$\mathrm{Upper}_{\mathrm{term}}$
1	214.89	3.90	Cu I	1.39	7.18	$4s^2\,^2D$	$5f\,^2F^0$
2	218.17	3.94	Cu I	0.00	5.68	$4s\,^2S$	$4p'\,^2P^0$
3	219.56	3.29	Cu II	8.78	14.43	$4p\,^3D^0$	$4d\,^3F$
4	219.95	2.88	Cu I	1.39	7.02	$4s^2\,^2D$	$4p''\,^2D^0$
5	221.45	2.40	Cu I	1.39	6.98	$4s^2\,^2D$	$4p''\,^2P^0$
6	224.20	2.45	Cu II	3.0	8.49	$4p$	$3D$
7	239.07	1.07	Al II	13.07	18.26	$4p\,^3P^0$	$10d\,^3D$
8	261.83	0.79	Cu I	1.39	6.12	$4s^2\,^2D$	$5p\,^2P^0$
9	284.02	0.68	Al I	4.02	8.39	$3d\,^2D$	$3d\,^2D^0$
10	306.34	0.92	Cu I	1.64	5.68	$4s^2\,^2D$	$4p'\,^2P^0$
11	308.21	1.34	Al I	0.00	4.02	$3p\,^2P^0$	$3d\,^2D$
12	309.27	1.88	Al I	0.01	4.02	$3p\,^2P^0$	$3d\,^2D$
13	324.75	1.42	Cu I	0	3.82	$4s\,^2S$	$4p\,^2P^0$
14	327.39	1.43	Cu I	0	3.39	$4s\,^2S$	$4p\,^2P^0$
15	329.05	1.05	Cu I	5.07	8.84	$4p'\,^4F^0$	$4d'\,^4F$
16	360.65	0.97	Ar I	11.62	15.06	$4s[1/2]^0$	$6p[1/2]$
17	394.40	1.27	Al I	0.00	3.14	$3p\,^2P^0$	$4s\,^2S$
18	396.15	1.76	Al I	0.01	3.14	$3p\,^2P^0$	$4s\,^2S$
19	402.26	0.64	Cu I	3.79	6.87	$4p\,^2P^0$	$5d\,^2D$
20	405.67	0.70	Al II	15.47	18.52	$3s4d\,^1D$	$3s15p\,^1P^0$
21	410.17	1.19	In I	–	3.02	$5s^25p\,^2P^0$	$5s^26s\,^2S_{1/2}$
22	415.85	1.18	Ar I	11.55	14.53	$4s[1/2]^0$	$5p[1\ 1/2]$
23	417.83	1.12	Ar II	16.64	19.61	$4s\,^4P$	$4p\,^4D^0$
24	419.07	0.74	Ar I	11.55	14.51	$4s[1/2]^0$	$5p[2\ 1/2]$
25	420.06	0.90	Ar I	11.55	14.50	$4s[1/2]^0$	$5p[2\ 1/2]$
26	422.26	1.22	Ar II	19.87	22.80	$4p\,^2P^0$	$5s\,^2P$
27	425.93	0.73	Ar I	11.83	14.74	$4s'[1/2]^0$	$5p'[1/2]$
28	426.62	0.70	Ar I	11.62	14.53	$4s[1/2]^0$	$5p[1\ 1/2]$
29	427.21	0.76	Ar I	11.62	14.52	$4s[1/2]^0$	$5p[11/2]$
30	430.01	0.76	Ar I	11.62	14.51	$4s'[1/2]^0$	$5p[2\ 1/2]$
31	433.35	0.89	Ar I	11.83	14.69	$4s'[1/2]^0$	$5p'[1\ 1/2]$
32	451.13	1.65	In I	0.27	3.02	$5s^25p\,^2P^0$	$5s^26s\,^2S_{1/2}$
33	484.22	1.18	Cu I	5.24	7.80	$4p'\,^4F^0$	$5s'\,^4D$
34	515.83	1.32	Cu I	5.69	8.09	$4p'\,^2P^0$	$5s'\,^2D$
35	516.22	1.13	Ar I	12.91	15.31	$4p[1/2]$	$6d[1/2]^0$
36	518.77	1.42	Ar I	12.91	15.30	$4p[1/2]$	$5d'[1\ 1/2]^0$
37	549.58	1.57	Ar I	13.08	15.33	$4p[2\ 1/2]$	$6d[3\ 1/2]^0$
38	555.87	1.46	Ar I	12.91	15.14	$4p[1/2]$	$5d[1\ 1/2]^0$
39	556.69	1.45	Se II				
40	594.92	2.00	Ar I	13.28	15.35	$4p'[1\ 1/2]$	$6d[1\ 1/2]$
41	603.21	2.25	Ar I	13.08	15.13	$4p[2\ 1/2]$	$5d[3\ 1/2]^0$

Cu II. For the resonance line of copper atom at 306.34 nm, the intensity growth was small (only about 1.3 times), perhaps because of self-absorption of plasma radiation. The intensity increase for the indium atomic lines at 410.17 and 451.22 nm was also small (about 1.1–1.2 times).

Concerning the spectral lines of aluminum atom at 308.21, 309.27, 394.40 (the resonance line), and

Table 2. **Identification of the most intensive spectral lines of aluminum atom and single-charged ion, as well as the molecular bands of decay products of the chalcopyrite molecule in overstressed nanosecond discharge at $p(\mathrm{Ar}) = 13.3$ kPa**

No.	$\lambda_{\mathrm{tab.}}$, nm	$I_{\mathrm{exp.}}$, a.u	Object	$E_{\mathrm{low.}}$, eV	$E_{\mathrm{up.}}$, eV	$\mathrm{Lover}_{\mathrm{term}}$	$\mathrm{Upper}_{\mathrm{term}}$
1	214.89	1.09	Cu I	1.39	7.18	$4s^2\,^2D$	$5f\,^2F^0$
2	218.17	0.47	Cu I	0.00	5.68	$4s\,^2S$	$4p'\,^2P^0$
3	219.56	0.53	Cu II	8.78	14.4	$4p\,^3D^0$	$4d\,^3F$
4	219.95	0.55	Cu I	1.39	7.02	$4s^2\,^2D$	$4p''\,^2D^0$
5	221.45	0.57	Cu I	1.39	6.98	$4s^2\,^2D$	$4p''\,^2P^0$
6	224.20	0.49	Cu II	3.0	8.49	$4p$	$3D$
7	239.07	0.82	Al II	13.07	8.78	$4p\,^3P^0$	$10d\,^3D$
8	261.83	0.44	Cu I	1.39	6.12	$4s^2\,^2D$	$5p\,^2P^0$
9	284.02	0.27	Al I	4.02	8.39	$3d\,^2D$	$3d\,^2D^0$
10	306.34	0.71	Cu I	1.64	5.68	$4s^2\,^2D$	$4p'\,^2P^0$
11	308.21	2.08	Al I	0.00	4.02	$3p\,^2P^0$	$3d\,^2D$
12	309.27	3.02	Al I	0.01	4.02	$3p\,^2P^0$	$3d\,^2D$
13	324.75	1.38	Cu I	0.00	3.82	$4s\,^2S$	$4p\,^2P^0$
14	327.39	1.04	Cu I	0.00	3.39	$4s\,^2S$	$4p\,^2P^0$
15	329.05	0.79	Cu I	5.07	8.84	$4p'\,^4F^0$	$4d'\,^4F$
16	360.65	0.64	Ar I	11.62	15.0	$4s[1/2]^0$	$6p[1/2]$
17	394.40	2.54	Al I	0.00	3.14	$3p\,^2P^0$	$4s\,^2S$
18	396.15	2.55	Al I	0.01	3.14	$3p\,^2P^0$	$4s\,^2S$
19	402.26	0.34	Cu I	3.79	6.87	$4p\,^2P^0$	$5d\,^2D$
20	405.67	0.58	Al II	15.47	18.52	$3s4d\,^1D$	$3s15p\,^1P^0$
21	410.17	1.01	In I	–	3.02	$5s^25p\,^2P^0$	$5s^26s\,^2S_{1/2}$
22	415.85	1.26	Ar I	11.55	14.53	$4s[1/2]^0$	$5p[1\ 1/2]$
23	417.83	0.5	Ar II	16.64	19.61	$4s\,^4P$	$4p\,^4D^0$
24	419.07	0.78	Ar I	11.55	14.51	$4s[1/2]^0$	$5p[2\ 1/2]$
25	420.06	1.51	Ar I	11.55	14.50	$4s[1/2]^0$	$5p[2\ 1/2]$
26	422.26	0.44	Ar II	19.87	22.80	$4p\,^2P^0$	$5s\,^2P$
27	425.93	0.73	Ar I	11.83	14.74	$4s'[1/2]^0$	$5p'[1/2]$
28	426.62	0.61	Ar I	11.62	14.53	$4s[1/2]^0$	$5p[1\ 1/2]$
29	427.21	0.72	Ar I	11.62	14.52	$4s[1/2]^0$	$5p[1\ 1/2]$
30	430.01	0.62	Ar I	11.62	14.51	$4s'[1/2]^0$	$5p[2\ 1/2]$
31	433.35	0.81	Ar I	11.83	14.69	$4s'[1/2]^0$	$5p'[1\ 1/2]$
32	451.13	1.51	In I	0.27	3.02	$5s^25p\,^2P^0$	$5s^26s\,^2S_{1/2}$
33	484.22	1.12	Cu I	5.24	7.80	$4p'\,^4F^0$	$5s'\,^4D$
34	515.83	0.49	Cu I	5.69	8.09	$4p'\,^2P^0$	$5s'\,^2D$
35	516.22	0.53	Ar I	12.91	15.31	$4p[1/2]$	$6d[1/2]^0$
36	518.77	0.50	Ar I	12.91	15.30	$4p[1/2]$	$5d'[1\ 1/2]^0$
37	549.58	0.65	Ar I	13.08	15.33	$4p[2\ 1/2]$	$6d[3\ 1/2]^0$
38	555.87	0.62	Ar I	12.91	15.14	$4p[1/2]$	$5d[1\ 1/2]^0$
39	556.69	0.60	Se II				
40	594.92	0.93	Ar I	13.28	15.35	$4p'[1\ 1/2]$	$6d[1\ 1/2]$
41	603.21	1.32	Ar I	13.08	15.13	$4p[2\ 1/2]$	$5d[3\ 1/2]^0$

396.15 nm, their intensities diminished from 1.4 to 2.3 times with the increasing argon pressure (Tables 1 and 2). For the ionic aluminum lines 239.07 and 405.67 nm Al II an increase of their intensities by about 1.3 times with the increasing argon pressure was registered (Tables 1 and 2). For the intensities of the spectral lines of argon atom at 549.58 and 594.92 nm, the intensity growth with the argon pres-

sure increase was the largest (by 2.4 and 2.2 times, respectively, see Tables 1 and 2). For the ionic argon lines 417.83 and 422.26 nm Ar II, the intensity increase was 2.3 and 2.8 times, respectively (Tables 1 and 2).

The electron concentration in discharges with the explosive (ectonic) mechanism of inserting the vapor of electrode material at atmospheric pressures of buffer gas can reach 10^7–10^8 m^{-3} [22]. Based on this fact, the formation mechanism of excited metal ions (copper and aluminum, Tables 1 and 2) in researched plasma can be governed by the processes of their electron excitation. The processes of electron-ion recombination begin only afterwards. A high efficiency of excitation of single-charged ions of transition metals (Zn, Cd, and others) in the ground energy state with slow electrons is evidenced by the results of systematic study of effective cross-sections of such processes that were carried out at the Institute of Electronic Physics of NAS of Ukraine (I.P. Zapisochnyi, O.B. Shpenyk, G.M. Gomonai, and others). For example, the corresponding effective electron excitation cross-sections for zinc ions reach a value of 10^{-12} m^2 [23].

The intensity increase of Al II spectral lines with increasing argon pressure may originate from the growing recombination efficiency of double-charged aluminum ions with electrons. The importance of recombination processes in microsecond spark-discharge plasma between aluminum electrodes is pointed out by the results of works [3, 24], where lines of double-charged ions were observed in plasma radiation spectra, in particular, it was the line 371.3 nm Al III [3]. In comparison with the argon atom and the chalcopyrite molecule, aluminum is an easily excitable and easily ionized element in examined plasma. Therefore, it is highly probable that single- and double-charge ions, primarily of aluminum, can be formed immediately in the course of microexplosions of natural inhomogeneities on the surface of aluminum electrode [25].

4. Numerical Simulation of Plasma Parameters

Besides the electrical and optical characteristics of overstressed nanosecond discharge plasma, it is important to determine such plasma parameters as the electron transport characteristics, the power of discharge losses for elastic and inelastic electron collisions with the argon and aluminum atoms and chalcopyrite molecules, and the ratio E/N between the electric field strength E and the total concentration N of the components in the experimental vapor-gas mixture. Numerical calculations of plasma parameters were performed assuming that the chalcopyrite molecule can be substituted by the copper atom, which is responsible for the main radiation emission characteristics of discharge and is the least bound entity in the chalcopyrite molecule. It was done because of the current absence of effective cross-section data for the interaction between electrons and the $CuInSe_2$ molecule. The concentration of copper vapor for simulation was chosen according to the data of work [28].

In order to calculate the parameters of plasma based on the mixtures of argon with aluminum and copper vapors, we used the standard program for solving the Boltzmann kinetic equation for the electron energy distribution function (EEDF). The application of this program assumes the presence of an electric field that is constant in time and space [27].

It is known that the time required for the electron energy distribution to become quasi-stationary is approximately equal to the relaxation time of the average electron energy [28, 29]

$$\tau = \frac{m v_e \varepsilon}{e^2 E^2},$$

where m is the electron mass, ε the average electron energy, e the electron charge, E the electric field strength, and v_e the frequency of elastic electron collisions with mixture atoms (argon, aluminum, and copper). The estimate of the τ magnitude for our experimental parameters gives a value of about 1×10^{-13} s, which is much shorter than the duration (about 10 ns) of voltage oscillations for overstressed nanosecond discharge between aluminum and chalcopyrite electrodes at argon pressures of 13.3 and 101 kPa obtained experimentally (Figs. 3 and 4, respectively). Therefore, we suppose that in our experiment, the standard *Bolsig+* software program for solving the Boltzmann kinetic equation for the EEDF [27] can be used.

The parameters of discharge plasma in mixtures of argon with aluminum and copper vapors were calculated numerically as complete integrals of the EEDFs. The latter were found by solving the Boltzmann kinetic equation in the two-term approximation. The EEDF calculations were performed using the software program [27]. The the database of the

latter, in particular, includes the effective cross-sections of electron interaction with the argon and copper atoms. The effective cross-sections of electron interaction with aluminum atoms were used in work [30]. On the basis of the calculated EEDFs, the main plasma parameters and their dependences on the reduced electric field (the ratio $E.N$ between the electric field strength E and the total concentration of argon atoms and the aluminum and copper impurity vapors N). The parameter E/N was varied within an interval of 1–2000 Td (i.e., 1×10^{-21}–2×10^{-18} V m^2), which included the experimental values. The integral of electron collisions with molecules and atoms took into account the following processes: elastic scattering of electrons by argon, aluminum, and copper atoms; excitation of the energy level of argon atom (a threshold energy of 11.50 eV); ionization of argon atom (a threshold energy of 15.80 eV); excitation of the energy levels of aluminum atom (threshold energies of 3.1707, 2.9032, 4.1463, 4.2339, 4.1296, and 5.1220 eV); ionization of aluminum atom (a threshold energy of 6.0000 eV); excitation of the energy levels of copper atom (threshold energies of 1.500, 3.800, and 5.100 eV); and ionization of copper atom (a threshold energy of 7.724 eV).

Figure 9 illustrates the dependences of the average electron energy on the reduced electric field strength for discharge plasma in the mixtures of argon at partial pressures of 101 and 13.3 kPa with impurities of aluminum and copper vapors at partial pressures of 100 Pa and 10 kPa. The average electron energy in the discharge increases linearly for all mixtures as the reduced electric field strength increases from 1 to 2000 Td: from 0.18 to 8.1 eV (curve *1*), from 0.47 to 17.68 eV (curve *2*), from 0.92 to 26.36 eV (curve *3*), and from 1.30 to 27.32 eV (curve *4*). Within an interval of 1–100 Td of the reduced electric field strength, the growth of the rate of its variation was larger in comparison with an interval of 100–2000 Td.

Table 3 contains the results of calculations of the electron transport characteristics – the average energies ε, the temperature T, the drift velocity V_{dr}, and the electron concentration N – for four mixtures of argon with aluminum and copper vapors and for the reduced field strengths that were 30, 50, and 150 ns after the discharge ignition. The average energy of discharge electrons in the gas-vapor mixture Ar–Al–Cu = 101 kPa : 100 Pa : 100 Pa reached at 30 ns after the pulse had begun ($E = 3\times10^7$ V/m, E/N = 1227 Td) was 17.8 eV, and 7.1 eV ($E = 3\times10^6$ V/m, E/N = 123 Td) at 150 ns after the pulse had begun. As the partial pressure of metal vapor increased, the average energy decreased to 9.6 and 2.8 eV, respectively.

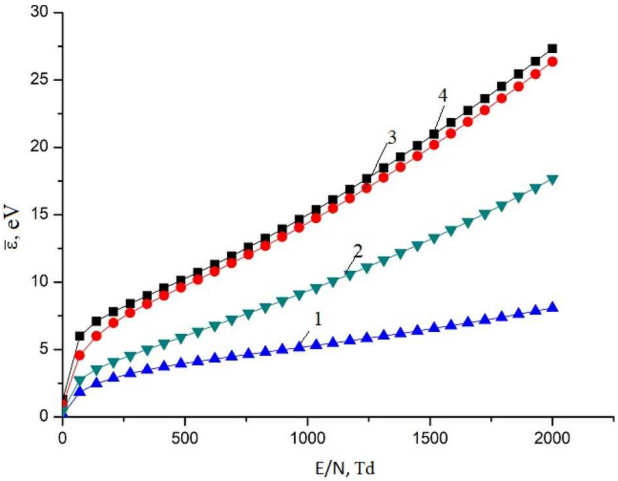

Fig. 9. Dependences of the average electron energy in the plasma of gas-vapor mixtures on the reduced electric field strength: (*1*) Ar–Al–Cu = 13.3 kPa : 10.0 kPa : 10.0 kPa, a total pressure of 33.3 kPa; (*2*) Ar–Al–Cu = 101 kPa : 10.0 kPa : 10.0 kPa, a total pressure of 121 kPa; (*3*) Ar–Al–Cu = 13.3 kPa : 0.1 kPa : 0.1 kPa, a total pressure of 13.5 kPa; (*4*) Ar–Al–Cu = 101 kPa : 0.1 kPa : 0.1 kPa, a total pressure of 101.2 kPa

Table 3. **Transport characteristics of electrons in discharge in the argon mixtures with aluminum and copper vapors for various partial-pressure ratios and at various moments after the discharge ignition**

τ, ns	E/N, Td	ε, eV	$T°$, K	$V_{\text{dr.}}$, m/s	N_e, m^{-3}
Mixture: Ar–Al–Cu = 101 kPa : 0.1 kPa : 0.1 kPa					
30	1227	17.8	206480	7.1×10^5	4.5×10^{19}
150	123	7.1	82360	9.6×10^4	6.5×10^{19}
Mixture: Ar–Al–Cu = 101 kPa : 10 kPa : 10 kPa					
30	1026	9.6	111360	4.2×10^5	7.6×10^{19}
150	103	2.8	32480	1.9×10^5	3.2×10^{19}
Mixture: Ar–Al–Cu = 13.3 kPa : 0,1 kPa : 0,1 kPa					
50	1875	24.5	284200	9.4×10^5	2.7×10^{19}
150	938	14.1	163560	5.2×10^5	9.8×10^{18}
Mixture: Ar–Al–Cu = 13.3 kPa : 10 kPa : 10 kPa					
50	746	4.7	54520	3.2×10^5	7.4×10^{19}
150	373	3.6	41760	2.6×10^5	1.2×10^{19}

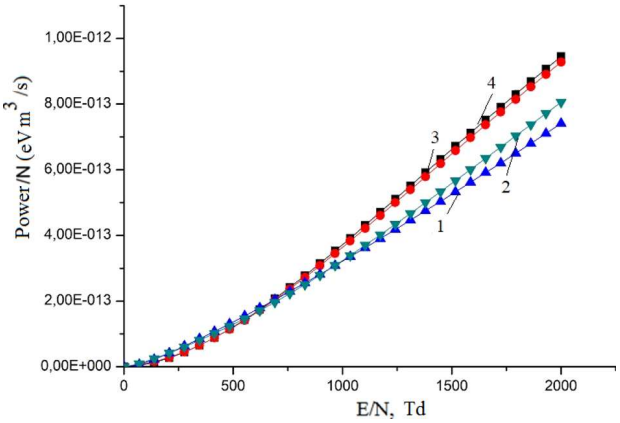

Fig. 10. Dependences of the specific discharge power losses at inelastic electron collisions with argon, aluminum, and copper atoms on the reduced electric field strength in the plasma of gas-vapor mixtures: (*1*) Ar–Al–Cu = 13.3 kPa : 10.0 kPa : 10.0 kPa, a total pressure of 33.3 kPa; (*2*) Ar–Al–Cu = = 101 kPa : 10.0 kPa : 10.0 kPa, a total pressure of 121 kPa;, (*3*) Ar–Al–Cu = 13.3 kPa : 0.1 kPa : 0.1 kPa, a total pressure of 13.5 kPa; (*4*) Ar–Al–Cu = 101 kPa : 0.1 kPa : 0.1 kPa, a total pressure of 101.2 kPa

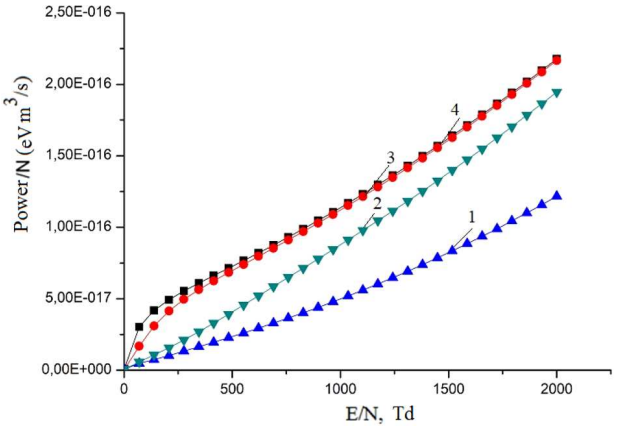

Fig. 11. The same as in Fig. 10, but for inelastic electron collisions with argon, aluminum, and copper atoms

The same dependence was observed for the electron temperature: it decreased with the increasing partial pressures of aluminum and copper vapors. As the partial argon pressure decreased to 13.3 kPa, the average electron energy for the mixture with partial pressures of metal vapors of 100 Pa was higher than for the discharge in the mixture with a partial argon pressure of 101 kPa: this quantity reached 24.5 and 14.1 eV, respectively. As the partial pressures of aluminum and copper vapors increased to 10 kPa and the partial argon pressure was 13.3 kPa, the average electron energy decreased to 4.7 and 3.6 eV, respectively. The electron temperature for lower partial argon pressures also decreased with the increasing partial pressures of aluminum and copper vapors.

The electron drift velocity behaved similarly to the average electron energy when the partial pressures of the gas-vapor mixture components changed. The maximum value of the electron drift velocity V_{dr} was 7.1×10^5 m/s for discharge in the mixture Ar–Al–Cu = 101 kPa : 100 Pa : 100 Pa. The electron concentration was maximum for discharge in the mixture Ar–Al–Cu = 101 kPa : 10 kPa : 100 kPa. Its value was 7.6×10^{19} m^{-3}.

In Figs. 10 and 11, the E/N-dependences of specific discharge power losses for inelastic and elastic, respectively, processes of electron collisions with the mixture components in the gas-discharge plasma are depicted. An increase of this parameter with the growing reduced electric field strength is observed in both cases. For inelastic processes, discharge losses in a E/N interval of 1–750 Td are approximately equal, and in an interval of 750–2000 Td, they vary within the same order of magnitude. For elastic processes, discharge losses begin to differ starting from E/N = 1 Td, and the difference increases with the

Table 4. **Specific discharge power losses for elastic and inelastic electron scattering processes in the argon mixtures with aluminum and copper vapors for various partial-pressure ratios and for the electric field strengths at various moments after the discharge ignition**

E/N, Td	Power/N (eV m^3/s)	
	Elastic	Inelastic
Mixture: Ar–Al–Cu = 101000 Pa : 100 Pa : 100 Pa		
1227	0.1363E-15	0.5109E-12
123	0.4186E-16	0.1345E-13
Mixture: Ar–Al–Cu = 101000 Pa : 1000 Pa : 1000 Pa		
1026	0.9111E-16	0.3390E-12
103	0.1068E-16	0.2454E-13
Mixture: Ar–Al–Cu = 133000 Pa : 100 Pa : 100 Pa		
1875	0.2007E-15	0.8906E-12
938	0.1090E-15	0.3452E-12
Mixture: Ar–Al–Cu = 133000 Pa : 1000 Pa : 1000 Pa		
746	0.3654E-16	0.2297E-12
373	0.1641E-16	0.8498E-13

Table 5. **Rate constants of spectral line excitation of aluminum and copper atoms in the argon mixtures with aluminum and copper vapors for the electric field strengths at various moments after the discharge ignition. E_{th} is the threshold excitation energy for the spectral lines of copper atom**

E/N, Td	Mixture: Ar–Al–Cu = 101000 Pa : 100 Pa : 100 Pa					
1227	Al	λ, nm	308.21	309.27	394.40	396.15
		k, m^3/s	1.619E-15	1.955E-15	2.357E-15	4.244E-15
	Cu	E_{th}, eV	1.5	1.5	3.8	5.1
		k, m^3/s	0.2835E-13	0.2248E-13	0.8894E-12	0.2374E-15
123	Al	λ, nm	308.21	309.27	394.40	396.15
		k, m^3/s	1.278E-15	1.814E-15	1.688E-15	3.317E-15
	Cu	E_{th}, eV	1.5 eV	1.5 eV	3.8 eV	5.1 eV
		k, m^3/s	0.2571E-13	0.1946E-13	0.4325E-12	0.1152E-15
E/N, Td	Mixture: Ar–Al–Cu = 101000 Pa : 10000 Pa : 10000 Pa					
1026	Al	λ, nm	308.21	309.27	394.40	396.15
		k, m^3/s	2.224E-15	1.929E-15	2.025E-15	3.785E-15
	Cu	E_{th}, eV	1.5	1.5	3.8	5.1
		k, m^3/s	0.2857E-13	0.2221E-13	0.6451E-13	0.1758E-15
103	Al	λ, nm	308.21	309.27	394.40	396.15
		k, m^3/s	6.078E-16	5.555E-16	9.438E-16	2.051E-15
	Cu	E_{th}, eV	1.5	1.5	3.8	5.1
		k, m^3/s	0.3763E-14	0.5107E-14	0.6451E-13	0.1758E-16
E/N, Td	Mixture: Ar–Al–Cu = 13300 Pa : 100 Pa : 100 Pa					
1875	Al	λ, nm	308.21	309.27	394.40	396.15
		k, m^3/s	0.2564E-13	1.957E-15	0.2452E-14	0.4441E-14
	Cu	E_{th}, eV	1.5	1.5	3.8	5.1
		k, m^3/s	0.2855E-13	0.2039E-13	0.9551E-12	0.2653E-15
938	Al	λ, nm	308.21	309.27	394.40	396.15
		k, m^3/s	0.2283E-14	0.1970E-14	0.2218E-14	0.4049E-14
	Cu	E_{th}, eV	1.5	1.5	3.8	5.1
		k, m^3/s	0.2950E-13	0.2322E-13	0.8064E-12	0.2121E-15
E/N, Td	Mixture: Ar–Al–Cu = 13300 Pa : 10000 Pa : 10000 Pa					
746	Al	λ, nm	308.21	309.27	394.40	396.15
		k, m^3/s	0.1245E-14	0.1114E-14	0.1306E-14	0.2722E-14
	Cu	E_{th}, eV	1.5	1.5	3.8	5.1
		k, m^3/s	0.1357E-13	0.9960E-14	0.1642E-12	0.4622E-16
373	Al	λ, nm	308.21	309.27	394.40	396.15
		k, m^3/s	0.5959E-15	0.5431E-15	0.9452E-15	0.2054E-14
	Cu	E_{th}, eV	1.5	1.5	3.8	5.1
		k, m^3/s	0.7009E-14	0.4981E-14	0.6170E-13	0.1680E-16

growth of the reduced electric field strength. In addition, the following regularity took place for power losses in the both cases of inelastic and elastic electron collisions with the mixture components; they were identical for discharge in the mixtures with lower partial vapor pressures of aluminum and copper. Such a regularity can be associated with higher electron energies in discharge in those mixtures (Table 3) and

close by values constants of inelastic and elastic processes in discharge in the mixtures with lower partial vapor pressures of aluminum and copper (Table 5).

Table 5 quotes the values of the rate constants for excitation of separate spectral lines of aluminum and copper atoms by discharge electrons in the examined gas-vapor mixtures for the magnitudes of the reduced electric field strength at 50, 150, and 300 ns after the discharge ignition (Figs. 3 and 4). These values vary within an interval of 0.1758×10^{-16}–0.9551×10^{-12} m^3/s for typical E/N values. The values obtained for copper atoms were higher than for aluminum ones in all researched mixtures. We also point out the increased values of the rate constants of spectral line excitation for both aluminum and copper atoms at 30–50 ns after the discharge ignition in comparison with the corresponding values at 150 ns. Such a behavior can be explained by different magnitudes of the reduced electric field strength at those time moments (see Figs. 3 and 4) and, accordingly, different average electron energies (Table 3), which is associated with different values of absolute effective cross-sections of inelastic electron collisions with copper and aluminum atoms. The effective cross-sections of inelastic electron collisions with copper atoms are larger than for aluminum ones [30], therefore the excitation rate constants for the spectral lines of copper atoms are also larger (Table 5).

5. Conclusions

To summarize, the study of the parameters of overstressed nanosecond discharge showed that a diffuse discharge is ignited between aluminum and chalcopyrite electrodes at the initial time moment if the argon pressure equals 13.3 or 101.3 kPa. Later, it contracts as is evidenced by the presence of a characteristic spark continuum of radiation in a spectral interval of 200–650 nm. The spark continuum of plasma radiation is most pronounced at an argon pressure of 101.3 kPa, which testifies to the discharge contraction already after the first half-wave of reflected voltage due to a mismatch between the plasma resistance and the resistance of the discharge supply system. Therefore, for the application of the diffuse discharge stage to be more efficient, it is necessary to ignite the discharge at partial argon pressures within an interval of 10–30 kPa.

The maximum pulsed electric discharge power reached a value of 4 MW, and the energy contribution to plasma per pulse was 423 mJ. The study of the spectral characteristics of plasma based on the gas-vapor mixtures Ar–Al–$CuInSe_2$ showed that the most intensive are the spectral lines of copper atom in an interval of 200–250 nm, and the spectral lines of indium and aluminum atoms and ions are observed in the longer-wavelength interval. The character of plasma radiation spectra does not speak in favor of any selective mechanisms giving rise to the formation of excited metal atoms and ions as a result of energy transfer from metastable atoms or argon molecules to aluminum, copper, or indium atoms. The following separate and most intensive lines in a spectral interval of 300–460 nm can be used to diagnose the sputtering of quaternary chalcopyrite films of the $CuIn_{1-x}Al_xSe_2$ type in real time: 307.38 and 329.05 nm Cu I; 410.17 and 451.13 nm In I; and 308.21, 309.27, 394.40, and 396.15 nm Al I. The presence of the main spectral lines of aluminum, copper, and indium in the plasma radiation spectra allows one to suppose the deposition of a thin film of quaternary chalcopyrite $CuIn_{1-x}Al_xSe_2$ beyond plasma, as it was implemented for ternary chalcopyrite $CuInSe_2$.

The study of the electron transport parameters, the discharge power losses for elastic and inelastic processes of electron collisions with the components of gas-vapor mixtures of argon with copper and aluminum atoms revealed an increase of the electron average energy and temperature in the mixtures with lower partial pressures of argon and aluminum and copper vapors, as well as their larger values for the reduced electric field strengths at 30 and 50 ns after the discharge ignition in comparison with the time moment $t = 150$ ns. The maximum values of the electron average energy and temperature were 24.5 eV and 284 200 K, respectively, for discharge in the gas-vapor mixture Ar–Al–Cu = 13300 Pa : 100 Pa : 100 Pa. The discharge power losses for elastic and inelastic electrons collisions with the components of gas-vapor mixtures had a similar behavior. They were larger for the reduced electric field strength at the moment of discharge ignition, being larger for inelastic electron collisions with the components of gas-vapor mixtures. A maximum value of $0.8906 \times \times 10^{-12}$ eV m^3/s was observed also for discharge in the mixture Ar–Al–Cu = 13300 Pa : 100 Pa : 100 Pa. Typical of discharges in all gas-vapor mixtures were also the larger values of the rate constants of spectral line excitation for both aluminum and cop-

per atoms at the initial moments of discharge ignition ($\Delta\tau = 30 \div 50$ ns) in comparison with the time moment $\tau = 150$ ns. This parameter varied within an interval of $0.1758 \times \times 10^{-16}$–$0.9551 \times 10^{-12}$ m^3/s.

For discharge in the mixture Ar–Al–Cu = = 13300 Pa : 100 Pa : 100 Pa, the rate constants of spectral line excitation for aluminum and copper atoms are substantial, which provides a higher intensity of the corresponding spectral lines emitted from the plasma discharge. Therefore they can be recommended for application at the diagnosis and sputtering of thin films on the basis of quaternary chalcopyrite in real-time mode.

1. A.K. Shuaibov, G.E. Laslov, Ya.Ya. Kozak. Emission characteristics of the cathode region of nanosecond discharge in atmospheric-pressure air. *Opt. Spectrosc.* **116**, 552 (2014).
2. A.K. Shuaibov, A.Y. Minya, M.P. Chuchman, A.A. Malinina, A.N. Malinin, T.Z. Gomoki, Y.Ch. Kolozvari. Optical characteristics of overstressed nanosecond discharge in atmospheric pressure air between chalcopyrite electrodes. *Plasma Res. Expr.* **1**, 015003 (2019).
3. L.F. Strelkov, A.A. Yankovskii. Variation of spectral-line intensity during spark discharge. *J. Appl. Spectrosc.* **19**, 605 (1973) (in Russian).
4. 4. V.V. Akhmadeev, L.M. Vasilyak, S.V. Kostyuchenko, N.N. Kudryavtsev, G.A. Kurkin. Spark breakdown of air by nanosecond voltage pulses. *Zh. Tekhn. Fiz.* **66**, 58 (1996) (in Russian).
5. A.K. Shuaibov, A.Y. Minya, A.A. Malinina, A.N. Malinin, V. V. Danilo, M.Yu. Sichka, I.V. Shevera. Synthesis of copper oxides nanostructures by an overstressed nanosecond discharge in atmospheric pressure air between copper electrodes. *Am. J. Mech. Mater. Eng.* **2**, 8 (2018).
6. D.V. Beloplotov, V.F. Tarasenko, M.I. Lomaev. Luminescence of atoms and ions of aluminum in pulseperiodic nanosecond discharge initiated by runaway electrons in nitrogen. *Opt. Atmosf. Okean.* **29**, 96 (2016) (in Russian).
7. A.M. Anpilov, E.M. Barkhudarov, Yu.N. Kozlov, I.A. Kossyi, M.A. Misakyan, I.V. Moryakova, M.I. Taktakishvili, N.M. Tarasova, S.M. Temchin. UV radiation of high-voltage multi-electrode surface discharge in gaseous medium. *Fiz. Plazm.* **45**, 268 (2019) (in Russian).
8. O.K. Shuaibov, O.Y. Minya, M.P. Chuchman, A.O. Malinina, O.M. Malinin, V.V. Danilo, Z.T. Gomoki. Parameters of nanosecond overnoltage discharge plasma in a narrov air gap between the electrodes containing electrode material vapor. *Ukr. J. Phys.* **63**, 790 (2018).
9. D.V. Beloplotov, V.I. Lomaev, D.A. Sorokin, V.F. Tarasenko. Blue and green jets in laboratory discharges initiated by runaway electrons. *J. Phys.: Conf. Ser.* **652**, 012012 (2015).
10. D.V. Beloplotov, M.I. Lomaev, V.F. Tarasenko. On the nature of the emission of blue and green jets in laboratory discharges initiated by a beam of runaway electrons. *Opt. Atmosf. Okean.* **28**, 349 (2015) (in Russian).
11. J. Lopez-Garcia, M. Placidi, X. Fontane, V. Izguierdo-Roca, M. Espindola *et al.* $CuIn_{1-x}Al_xSe_2$ thin film solar cells with depth gradient compositions prepared by selenization of evaporated metallic precursors. *Solar Energ. Mater. Solar Cells* **132**, 245 (2015).
12. O.K. Shuaibov, A.O. Malinina, O.M. Malinin. *New Gas-Discharge Methods for Obtaining Selective Ultraviolet and Visible Radiation and Synthesizing Nanostructures of Transition Metals* (Uzhgorod National University Publishing House "Goverla", 2019) (in Ukrainian).
13. A.K. Shuaibov, A.I. Minya, A.A. Malinina, R.V. Gritsak, A.N. Malinin. Characteristics of the nanosecond overvoltage discharge between $CuInSe_2$ chalcopyrite electrodes in oxygen – free gas media. *Ukr. J. Phys.* **65**, 400 (2020).
14. V.F. Tarasenko. *Runaway Electrons Preionized Diffuse Discharge* (Nova Science Publishers Inc., 2014).
15. A. Shuaibov, A. Minya, A. Malinina, A. Malinin, Z. Gomoki. Synthesis of aluminum oxide nanoparticles in overstressed nanosecond discharge plasma with the ectonic sputtering mechanism of aluminum electrodes *Highlight. BioSci.* **32**, 20211 (2020).
16. A.R. Striganov, N. S. Sventitskii. *Tables of Spectral Lines of Neutral and Ionized Atoms* (IFI/Plenum, 1968).
17. *NIST Atomic Spectra Database Lines Form* [https://physics.nist.gov/PhysRefData/ASD/lines_form.html].
18. R.W.B. Pearse, A.G. Gaydon. *The Identification of Molecular Spectra* (Chapman and Hall, 1976).
19. I.E. Kacher, A.K. Shuaibov, M.Yu. Rigan, A.I. Dashchenko. Optical diagnostics of laser evaporation of polycrystalline compound $CuInS_2$. *Teplofiz. Vys. Temp.*.**40,** 880 (2002) (in Russian).
20. O.K. Shuaibov, M.P. Chuchman, L.L. Shimon, I.E. Kacher. Research of optical characteristics and parameters of laser plasma of $CuInS_2$ polycrystalline fusion mixture and its components. *Ukr. Fiz. Zh.* **48**, 223 (2003) (in Ukrainian).
21. A.K. Shuaibov, A.Y. Minya, Z.T. Gomoki, R.V. Hrytsak, A.A. Malinina, A.N. Malinin, V.M. Krasilinets, V.M. Solomon. Characteristics and parameters of jverstressed nanosecond discharge plasma between electrodes from chalcopyrite ($CuInSe_2$) in argon at atmospheric pressure. *Surf. Eng. Appl. Electrochem.* **56**, 474 (2020).
22. D. Levko, L.L.Raja. Early stage time evolution of a dense nanosecond microdischarge use in fast switching applications. *Phys. Plasmas* **22**, 123518 (2016).
23. A.N. Gomonai. Radiative decay np^2 autoionization states under dielectronic recombination of the Zn^+ and Cd^+ ions. *J. Appl. Spectrosc.* **82**, 17 (2015).
24. J.P. Walters, H.V. Malmstadt. Emission characteristics and sensitivity in a high-voltage spark discharge. *Analyt. Chem.* **37**, 1484 (1965).
25. G.A. Mesyats. Ecton or electron avalanche from metal. Usp. Fiz. Nauk **38**, 567 (1995) (in Russian).

26. A.S. Pashchina, A.V. Efimov, V.F. Chinnov. Optical research of multicomponent capillary discharge plasma. Supersonic outflow mode. *Teplofiz. Vys. Temp.* **55**, 669 (2017) (in Russian).
27. *BOLSIG+* [https://nl.lxcat.net/solvers/BOLSIG+].
28. Yu.P. Raizer, *Gas Discharge Physics* (Springer, 1997).
29. M.M. Mkrtchyan. Kinetics of a gas-discharge XeF excimer laser. *Sov. J. Quant. Electron.* **9**, 967 (1979).
30. L.L. Shymon. An effect of autoionising states on population of energy levels of atoms in aluminium subgroup. *Nauk. Visn. Uzhgorod. Univ. Ser. Fis.* **20**, 55 (2007) (in Ukrainian).

Received 20.11.20.
Translated from Ukrainian by O.I. Voitenko

О.К. Шуаібов, О.Й. Миня,
А.О. Малініна, Р.В. Грицак, О.М. Малінін

ОПТИЧНІ ХАРАКТЕРИСТИКИ І ПАРАМЕТРИ ПЛАЗМИ ПЕРЕНАПРУЖЕНОГО НАНОСЕКУНДНОГО РОЗРЯДУ МІЖ ЕЛЕКТРОДАМИ З АЛЮМІНІЮ ТА ХАЛЬКОПІРИТУ ($CuInSe_2$) В АРГОНІ

Приведено оптичні характеристики і параметри перенапруженого наносекундного розряду в аргоні між електродами з алюмінію і халькопіриту ($CuInSe_2$) при $p(Ar) = 13{,}3$ і 101 кПа. Внаслідок мікровибухів природних неоднорідностей на робочих поверхнях електродів в сильному електричному полі в плазму вносяться як пари алюмінію, так і пари халькопіриту, що створює передумови для синтезу за межами розряду тонких плівок четверного халькопіриту – $CuAlInSe_2$. Досліджено імпульси напруги і струму на розрядному проміжку величиною $d = 1 \cdot 10^{-3}$ м (розміри наведено в системі СІ), а також імпульсний енергетичний внесок у плазму. Ретельно досліджено спектри випромінювання плазми, що дозволило встановити основні продукти розпаду молекули халькопіриту та енергетичні стани атомів і однозарядних іонів алюмінію, міді і індію, в яких вони утворюються в розряді. Виявлено реперні спектральні лінії атомів і іонів алюмінію, міді і індію, які можуть бути використані для контролю за процесом напилення тонких плівок четверного халькопіриту. Методом числового моделювання параметрів плазми перенапруженого наносекундного розряду на основі парів алюмінію і халькопіриту, шляхом розв'язку кінетичного рівняння Больцмана для функції розподілу електронів за енергіями розраховано температуру і концентрацію електронів у розряді, питомі втрати потужності розряду на основні електронні процеси і константи швидкості електронних процесів в залежності від величини параметра E/N (де E – напруженість електричного поля, N – загальна концентрація суміші парів алюмінію та аргону.

Ключові слова: перенапружений наносекундний розряд, алюміній, халькопірит, аргон.